Atomic and Nuclear Physics

Atomic Shell
Optical Pumping (Anomalous Zeeman Effect)

LD
Physics
Leaflets

P6.2.8.4

Optical pumping: measuring and observing the Zeeman transitions in the ground states of Rb-87 as a function of magnetic flux density B

Objects of the experiment

■ Observation of Zeeman transitions in ground states of ^{87}Rb inside various magnetic fields.

■ Determination of the nuclear spin g_I of ^{87}Rb.

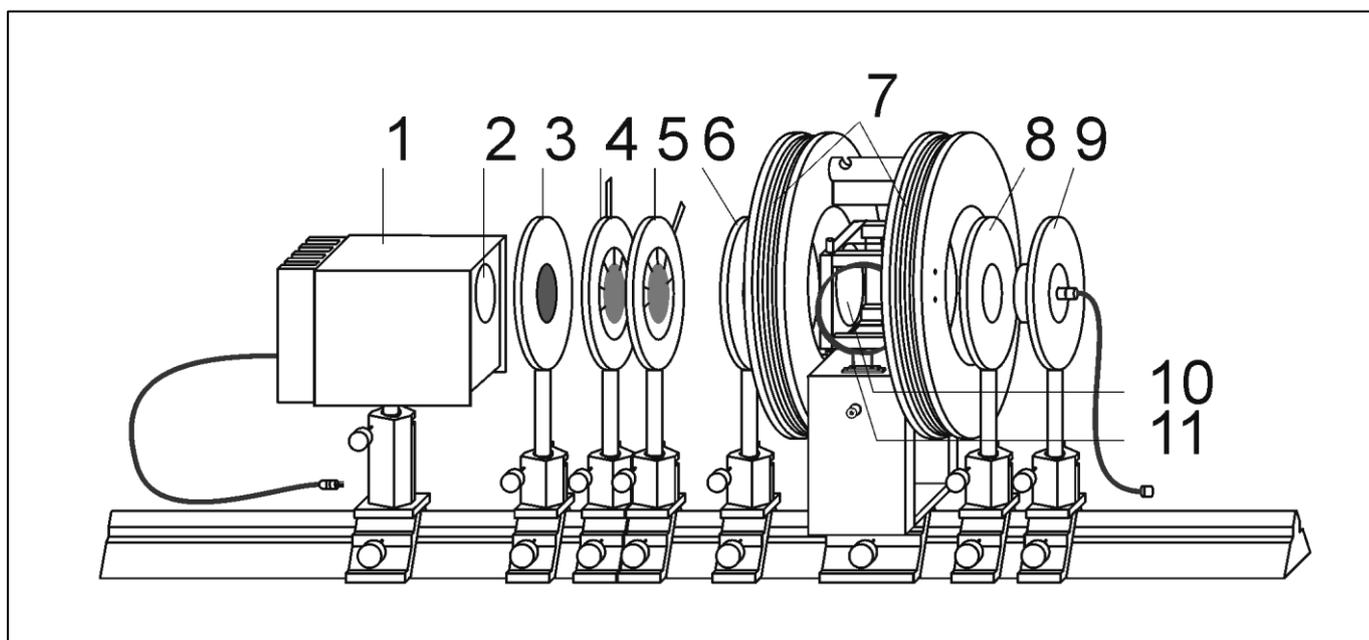■ Observation of how lines can cross over and swap positions in the frequency spectrum.

Fig 1: Optical and magnetic components for the experiment "optical pumping"

1	Rubidium high-frequency lamp	6	Lens on brass stem, f = + 100 mm
2	Lens, f = + 50 mm	7	Helmholtz coils, pair
3	Line filter, 795 nm	8	Lens on brass stem, f = + 50 mm
4	Polarisation filter for red radiation	9	Silicon photodetector
5	Quarter-wavelength plate, 200 nm	10	Absorption chamber with rubidium absorption cell
		11	High-frequency coils

Principles

Optical pumping [1,2,3] permits spectroscopic analysis of atomic energy states in an energy range not accessible to direct optical observation.

In weak magnetic fields, the differences in the population number between the Zeeman levels in the ground state of ^{87}Rb are extremely slight, as the energy interval is less than 10^{-8} eV. Optical pumping produces a population which deviates greatly from the thermal equilibrium population. To accomplish this, rubidium vapour is irradiated in an absorption cell with the circularly polarised component of the D_1 light from a rubidium lamp. The population of the Zeeman level depends on the polarity of the incident light. When the cell is irradiated with a high-frequency alternating magnetic field, we observe a change in the transparency of the rubidium vapour for rubidium-D_1 light.

A rubidium high-frequency lamp is used as the pumping light source. Rubidium atoms in a glass ampoule are excited in the electromagnetic field of an HF transmitter.

The combination of an interference filter, a polarisation filter and a quarter-wavelength plate separate the desired circularly polarised component of the D_1 line from the emission spectrum of the light source. Depending on the position of the quarter wavelength plate, we obtain either σ^+ or σ^- polarisation.

A system of convex lenses focuses the pumping light on the centre of the absorption cell (also filled with rubidium vapour) and the transmitted component of the pumping light on a photodetector (cf. Fig. 5).

The Zeeman magnetic field is generated using Helmholtz coils. Depending on the polarity of the coil current, the field lines are oriented either parallel or anti-parallel to the optical radiation.

Using the high-frequency coil pair, it is possible to generate a high-frequency alternating field perpendicular to the Zeeman magnetic field. When its frequency corresponds to the energy difference of two adjacent Zeeman levels, transition between the levels can occur. The populations of the Zeeman levels, and thus the transparency of the rubidium vapour, change.

To determine the change in transparency, the intensity of the transmitted light is measured using a silicon photodetector. A current/voltage converter amplifies its output signal. The transmitted intensity is recorded as a function of the frequency of the irradiated high-frequency field. This frequency is varied in a linear fashion between a user-definable start frequency and stop frequency using a function generator.

Physical principles

In its ground state, rubidium, like all alkali metals, has a total spin of the electron shell with the spin quantum number $J = \dfrac{1}{2}$. The ground state thus splits into two hyperfine states with the total angular momenta $F = I + \dfrac{1}{2}$ and $F = I - \dfrac{1}{2}$ respectively.

In the magnetic field, the hyperfine states are each split into $2F+1$ Zeeman levels with the magnetic quantum numbers $m_F = -F, \ldots, F$. Fig. 1 shows an example of the level diagram for ^{87}Rb.
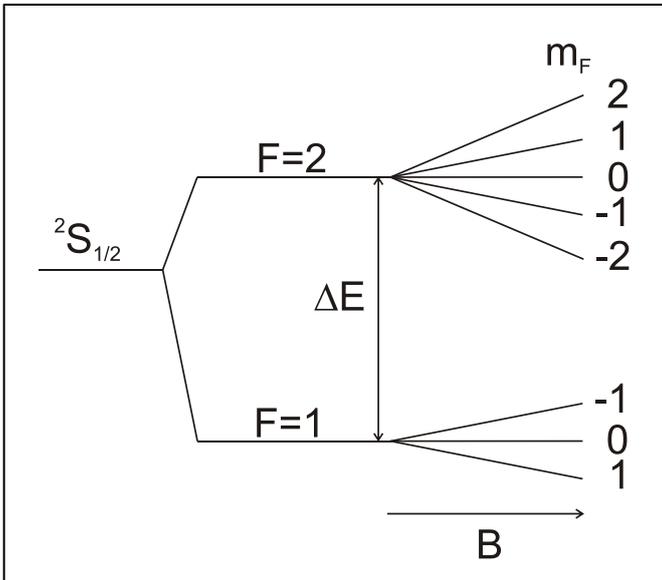

Fig. 1: Schematic representation of Zeeman levels in the ground state of ^{87}Rb Hyperfine splitting ΔE and Zeeman splitting are not drawn to scale.

The energy E of the Zeeman levels can be calculated for the magnetic fields used here with the help of the Breit-Rabi formula [4,5]:

For $F = I \pm \dfrac{1}{2}$

$$E(F, m_F) = -\frac{\Delta E}{2(2I+1)} + \mu_K g_I B m_F \pm \frac{\Delta E}{2}\left(1 + \frac{4m_F}{2I+1}\xi + \xi^2\right)^{\frac{1}{2}}$$

where $\xi = \dfrac{g_J \mu_B - g_I \mu_K}{\Delta E} B$ (I)

F :   Total angular momentum

I :   Nuclear spin

J :   Angular momentum of the electron shell

m_F :   Magnetic quantum number of the total angular momentum F

g_I :   g-factor of the nucleus

g_J :   g-factor of the electron shell

ΔE :   Hyperfine structure spacing

μ_B :   Bohr magneton

μ_K :   Nuclear magneton

B :   Magnetic flux density

The positions of the energy levels as given by equation (I) for ^{87}Rb are shown in Fig. 3. The calculations have also been made extending up to very strong magnetic fields in order to illustrate the change-over between the Zeeman effect and the Paschen-Back effect, even though it is only possible to create fields of 1 mT in this experiment.

It is possible for optical transitions to occur from the split Zeeman levels of the ^{2}S$_{1/2}$ ground state to the ^{2}P$_{1/2}$ and ^{2}P$_{3/2}$ levels. When irradiated with σ^+ pumping light, the Zeeman levels within a hyperfine state which have positive quantum numbers m_F become enriched at the expense of the levels with negative quantum numbers. In the ground state ^{87}Rb, for example, the level with $F = 2$, $m_F = +F$ has the greatest population. The result is a population which deviates from the thermal equilibrium population. With σ^- pumping light, the situation is just the opposite, as the Zeeman levels with negative quantum numbers predominate.

The energy difference between adjacent m$_F$ Zeeman levels in a magnetic field of 1 mT corresponds to the high-frequency range of about 7 MHz. When irradiated with a linearly polarized alternating magnetic field of the correct frequency, more transitions take place from a higher Zeeman level m_F to the next lowest level with $m_F - 1$ than in the other direction.

Due to the different population numbers, when a high-frequency field is applied, more atoms capable of absorbing the pumping light are available and the amount of light transmitted drops. The result is that when a resonant high-frequency field is applied, there is a reduction in optical transmission. By this indirect means, it is possible to demonstrate the effects of the applied high-frequency field in a way which is orders of magnitude more sensitive than direct measurement of the HF absorption.
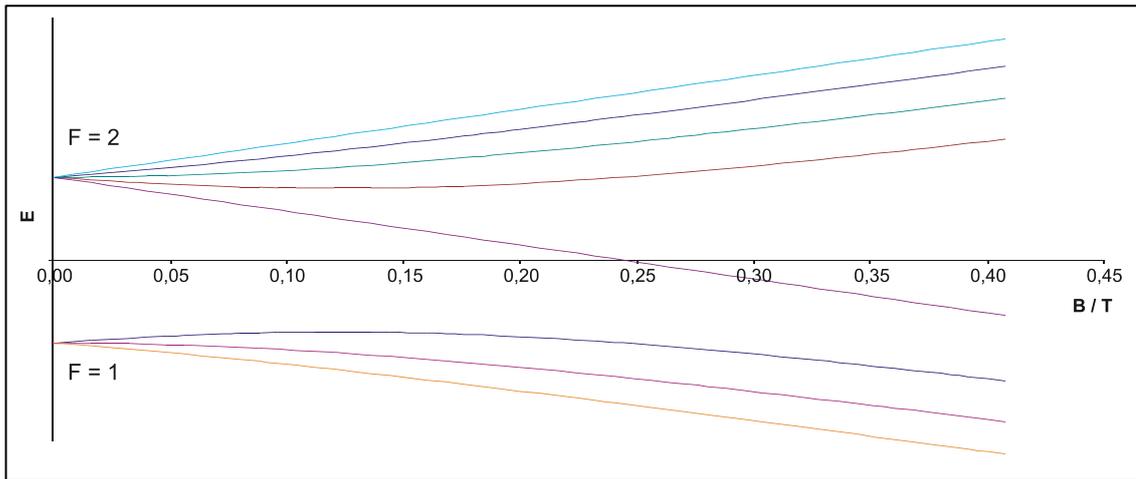
Fig. 2:   Energy level of $^2S_{1/2}$ ground state of ^{87}Rb

Regardless of the channel used for the demonstration, the frequency f for these transitions is given by

$$f(m_F \leftrightarrow m_F - 1) = \pm \frac{\mu_K g_I B}{h}$$

$$+ \frac{\Delta E}{2h} \left(\left(1 + \frac{4m_F}{2I+1} \xi + \xi^2 \right)^{\frac{1}{2}} - \left(1 + \frac{4(m_F - 1)}{2I+1} \xi + \xi^2 \right)^{\frac{1}{2}} \right)$$

(II)

The frequency f of the transitions is largely linearly dependent on the magnetic field B when the fields are not very strong, as would be expected for the Zeeman effect. The lines for the individual transitions between m$_F$ states move with increasing field strength B to increasingly higher frequencies and the separation between them also increases.

In order to show the splitting of the lines which is solely due to the field relative to their own centre, a fixed linear term is

movement of the central frequency of the line (for ^{87}Rb, for example, this is 6.99 MHz/mT). The splitting between the individual lines in the kHz range which results from this is shown in Fig. 4.

It can be seen that as the magnetic field changes, the lines of the F=1 and F=2 groups actually cross over and swap positions.

If similar m$_F$ transitions in various F states are considered, these are indistinguishable in the lower part of formula (II). This allows for one simple way of determining the nuclear Landé g-factor g from the top part of equation (II).

Fig. 3:   Relative energy differences between energy levels from Fig. 2. A linear term of 6.99 MHz/mT is subtracted from all transitions. These lines mark the positions of spectra to be measured later on.
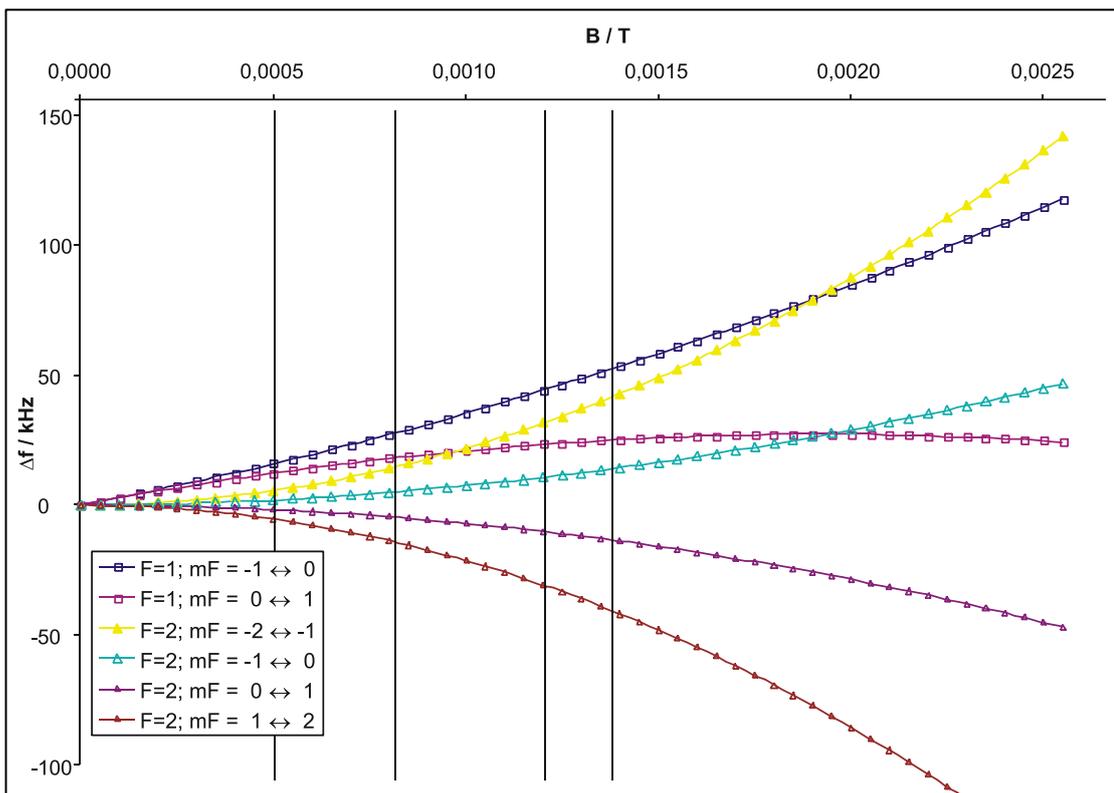
subtracted from all the transitions which represents the move-

Safety notes

Protecting individuals

Danger of scalding: hot water can leak from insecurely fastened or defective water tubing between the circulation thermostat and the absorption chamber:

– Use only silicon tubing of the specified diameter.

– Clamp the tubes in the holder between the Helmholtz coils and secure them against slippage.

Protecting the equipment

The absorption chamber is made of acrylic glass and can be destroyed by heat:

– Fill the absorption chamber with distilled water only.

– Do not heat the absorption chamber above 80°C.

– Never clean the absorption chamber with solvents.

The uniformity of the Helmholtz field is impaired if the Helmholtz coil cores become deformed:

– Protect Helmholtz coils from shocks or knocks.

The HF transmitter in the rubidium high-frequency lamp can be destroyed by excessive voltage levels:

– Only operate the rubidium high-frequency lamp with the optical pumping supply unit.

For best experiment results

The experiment setup is sensitive to interfering magnetic fields:

– Keep all power supplies and measuring instruments as far away from the experiment setup as possible.

– Remove ferromagnetic materials or devices which generate magnetic fields from the vicinity of the experiment setup.

– Use only lenses on brass stems (460 021 and 460 031).

Room lighting can drown out the measurement signal at the silicon photodetector. External light unnecessarily raises the DC component of the photodetector signal:

– Switch off the electric lighting in the room.

– Prevent the incidence of external light.

– Darken the experiment room.

– Turn the reflective side of the line filter so that it faces the rubidium high-frequency lamp.

The direction of flow of the heating water in the absorption chamber is determined by the experiment setup:

– Make sure the water inlets and outlets are connected in the proper direction.

High frequencies interfere with voltage-sensitive measuring instruments:

– Only use the rubidium high-frequency lamp when it is fully assembled.

Equipment list

1 Rubidium high-frequency lamp 558 823
1 Pair of Helmholtz coils on stand rider 558 826
1 Absorption chamber
 with rubidium absorption cell 558 833
1 Silicon photodetector 558 835
1 I/V converter for silicon photodetector 558 836

1 Supply unit for optical pumping 558 814
1 Function generator, 1mHz - 12 MHz.................522 551
1 DC power supply, 0...±15 V 521 45
1 Circulation thermostat, +30°C to +100°C..........666 768
1 Digital storage oscilloscope, e.g. 575 294
1 Plug-in power unit, 9,2V-, regulated 530 88
1 Digital/analog multimeter MetraHit Pro 531 281
1 Two-way switch 504 48

1 Optical bench, standardised profile, 1m 460 32
1 Line filter, 795 nm...468 000
1 Polarisation filter for red radiation 472 410
1 Quarter-wavelength plate, 200 nm 472 611
1 Lens on brass stem, f = +50 mm 460 021
1 Lens on brass stem, f = +100 mm 460 031
6 Optical riders 60/34 ....460 370
1 Optical rider 95/50 ....460 374

1 Silicone tube, 5 m long, 6.0x2.0 ....688 115
4 Connecting leads, black, 50 cm.........................501 28
2 Connecting leads, black, 200 cm.......................501 38
3 BNC cables, 1 m...501 02
1 BNC cable, 2 m 501 022
2 Canisters of water, pure, 5 l..............................675 3410

The following applies for the Helmholtz coils:

$$B = \left(\frac{4}{5}\right)^{3/2} \frac{\mu_0 N}{r_{eff}} I$$

(III)

where, for example,

r_{eff} = 116 mm

N=210

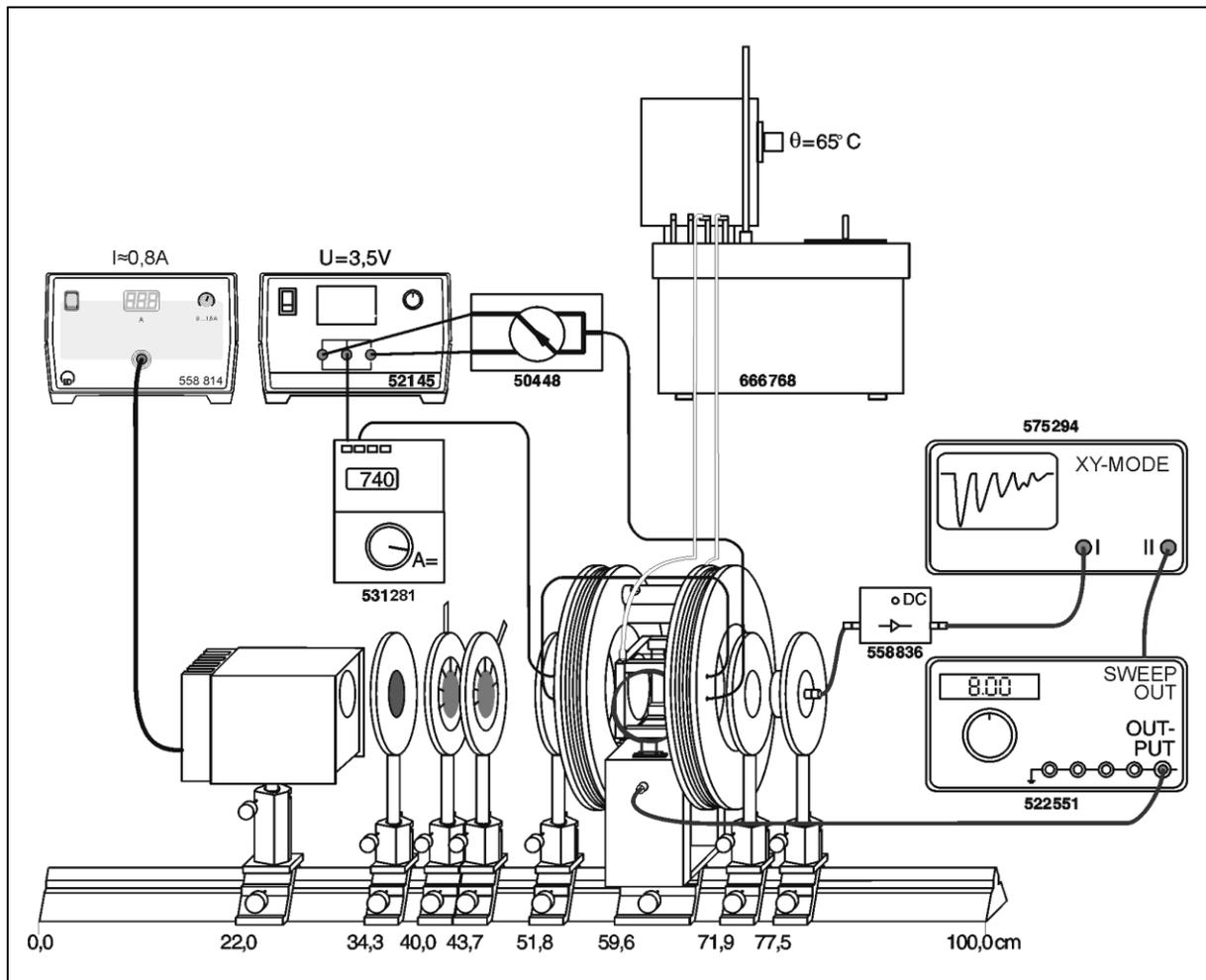results in a field

B= 1.205 mT for I = 0.740 A

Fig. 4: Overview diagram of the entire experiment setup. Position specifications are measured from the left edge of the optical riders.

Setup

Optical and electrical setup

– Set up the optical and magnetic components on the optical bench with standardised profile (460 32), as shown in **Fehler! Verweisquelle konnte nicht gefunden werden.** and Fig. 5.

– Connect the rubidium high-frequency lamp with the supply unit for optical pumping (558 814).

– Connect the Helmholtz coils and the multimeter (531 281) in series to the power supply (521 45).

– Insert the two-way switch (504 48) in the circuit to permit easy reversal of the magnetic field.

– Connect the output of the function generator (522 551) to the HF coils.

– Connect the photodetector output to channel I of the oscilloscope (575 294) via the I/V converter (558 836).

– Connect the sweep output, Sweep Out, on the function generator to channel II of the oscilloscope.

Warming up the system

– Using silicone tubing, set up a heating water circuit between the absorption chamber and the circulation thermostat (666 768) as shown in Fig. 5.

– Switch on the circulation thermostat and set the temperature θ to 65°C.

– Switch on the supply unit for optical pumping and set the operating current to about 0.8 A (cf. instruction sheet for the rubidium high-frequency lamp 558 823).

– Switch on the stabilised power supply.

– Wait at least 15 min. until the operating temperature is reached.

If the light output of the rubidium high-frequency lamp is unstable:

– Increase the operating current by about 0.1 A.

Initial optical adjustment

– Remove the optical riders with line filter, polarisation filter and quarter wavelength plate from the optical bench.

– Remove the absorption chamber from the stand rider for the Helmholtz coils.

– Hold a white piece of paper in place of the absorption cell at the midpoint between the Helmholtz coils.

– Move the lens (6) and the rubidium high-frequency lamp so that the smallest possible evenly illuminated light spot is obtained (cf. Fig. 5).

– Remove the optical rider with the silicon photodetector from the optical bench.

– Using the piece of paper, find the point with the smallest evenly illuminated light spot.

– Move lens (8) to improve the illumination (cf. Fig. 5).

– Set up the silicon photodetector at the point where the piece of paper is.

When the initial adjustment is complete:

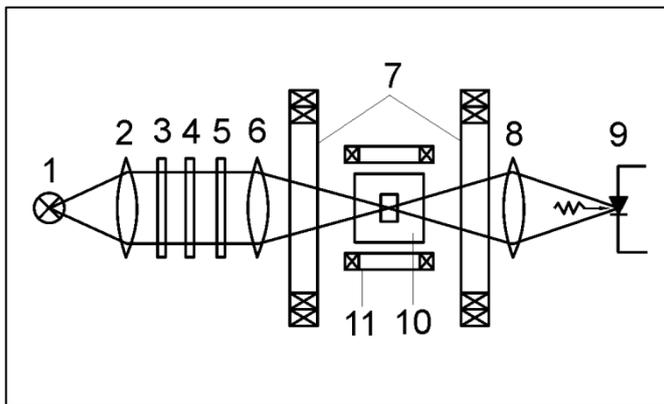– Set up the components that were previously removed on the optical bench again.

Fig. 5:   Schematic representation of the radiation path for optical pumping. For designations of the optical and magnetic components see **Fehler! Verweisquelle konnte nicht gefunden werden.**

Fine adjustment

To obtain the maximum light intensity at the silicon photodetector:

– Set the I/V converter to DC coupling

– Observe the photodetector signal at the oscilloscope.

– Alternately adjust the height and position of the rubidium high-frequency lamp, lenses (6) and (8), the absorption chamber and the silicon photodetector so as to obtain the maximum photodetector signal.

– If necessary, use the offset potentiometer of the I/V converter to bring the signal back to the middle of the oscilloscope screen.

Settings

Oscilloscope:

      Channel I: 10-20 mV/DIV. (DC)

I/V converter:

      Toggle switch: DC

Finding the absorption signal

For ^{87}Rb the frequencies of the Zeeman transitions in the ground state in a Helmholtz field of 1.2 mT (coil current 740 mA) are around 8 MHz. When the setup is carefully adjusted, the absorption signal reaches an amplitude of approximately 20 mV (higher signals could be achievable if the operating current of the rubidium lamp were increased, but this also would reduce the lifespan of the lamp):

– Set the polarisation filter to 0° and the quarter wavelength plate to +45° or -45°.

– Set the desired operating mode and frequency range on the function generator.

– Start the function generator by pressing the button labelled MANUAL.

– Vary the Helmholtz coil current until the maximum (negative) absorption signal appears on the oscilloscope.

– If necessary, set the toggle switch of the I/V converter to AC or use the offset potentiometer of the I/V converter to bring the signal back to the middle of the oscilloscope screen.

– Maximise the absorption signal by changing the operating parameters of the rubidium high-frequency lamp.

Settings

Polarisation filter:

      Angle: 0°

Quarter wavelength plate:

      Angle: +45° or –45°

I/V converter:

      Toggle switch: DC

Oscilloscope:

      Operating mode: X-Y Mode

      Channel I: ≥10 mV/DIV (DC)

      Channel II: 0.5 V/DIV. (DC)

Function generator:

      Function: ~ (Sine)

      Amplitude: Middle position

      Attenuation: 20 dB

      DC -offset: 0 V (DC button pressed)

      Sweep button: Pressed

      Mode*:   'C u

      Stop*:   8.5 MHz

      Start*:   7.5 MHz

      Period*:   100 ms approx. (fast sweep)

* Press button and set desired value with knob

Measuring

Preparation

Finding the signal:

– Operate the oscilloscope in XY-mode.

– Switch off the oscilloscope's storage mode.

– If necessary, switch off the sensitivity of oscilloscope channel I.

– Set the toggle switch of the I/V converter to DC.

– Set the start and stop frequencies on the function generator (f_A = 9,0 MHz, f_E = 9,2 MHz).

– Switch the function generator to a period of 100 ms (fast sweep).

– Start the function generator by pressing the button labelled MANUAL.

– Set the Helmholtz coil current I ≈ 0,8 A and vary it until an absorption signal can be seen on the oscilloscope screen.

Oscilloscope storage mode:

– Switch on the storage mode of the oscilloscope.

– Press the START button on the function generator.

– Set the horizontal deflection of the oscilloscope to x_A = 1.0 divisions.

– Press the STOP button of the function generator.

– Set the horizontal deflection of the oscilloscope to x_E = 9.0 divisions.

Fine adjustment:

– Start the function generator by pressing the button labelled MANUAL.

– Switch the function generator to a period of 10 ms (slow sweep).

– Switch the vertical deflection of the oscilloscope to sensitive..

– Turn the quarter wavelength plate back and forth between +45° and −45° and check whether all lines of the absorption spectrum appear on the oscilloscope screen.

– If necessary, readjust the Helmholtz coil current *I* or the start frequency f_A and stop frequency f_E accordingly.

Procedure

Note: with σ^+-polarisation, the absorption line with the lowest frequency is the most intense.

First run:

– Set the quarter-wavelength plate to σ^+ polarisation.

– Start the function generator by pressing the button labelled MANUAL.

– Wait until the absorption spectrum has been completely recorded.

– Stop recording the absorption spectrum.

– Determine the position *x* of the absorption lines on the oscilloscope screen.

– Determine the amplitude *V* of the absorption lines.

– Check the start frequency f_A and the stop frequency f_E .

– Check the Helmholtz coil current *I*.

Subsequent runs:

Vary the coil current.

Calculate the resulting magnetic field using equation (III)

(B/I= 1.628 mT/A)

Estimate the approximate positions of the high-frequency transitions

(f/B = 7 MHz/mT)

Set (f-0.1 MHz) as the start value and (f+0.1 MHz) as the stop value on the function generator in each case and carry out a measurement.

Due to the change in the magnetic polarisation of the ground state in varying magnetic fields, the way the spectra depend on the power will also change. The weaker the magnetic field, the less high-frequency energy will be required.

Settings

Oscilloscope:

Operating mode:	X-Y mode
	Storage mode
Channel I:	10 mV/DIV. (DC)
Channel II:	>0.5 V/DIV. (DC)
Recording range:	1.0 division - 9.0 divisions
Time base:	1 s/DIV

Function generator::

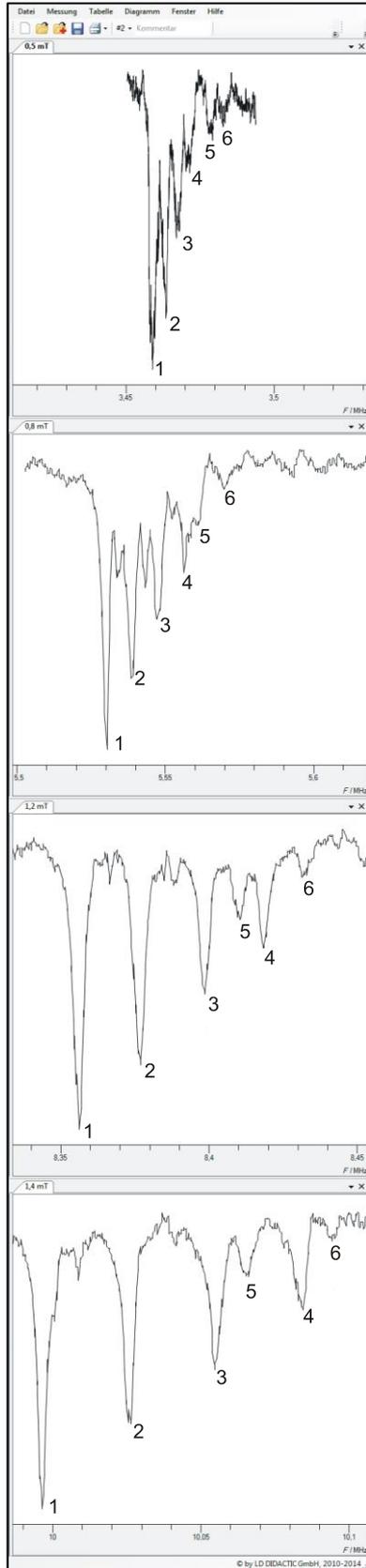|	
Stop:	f+0.1 MHz
Start:	f-0.1 MHz
Period:	10 s (slow sweep)
Amplitude:	3rd division
Attenuation:	20 dB

Measuring example

Fig. 6: Zeeman transitions for ⁸⁷Rb in various magnetic fields, top to bottom: 0.5 mT / 0.79 mT / 1.2 mT / 1.44 mT
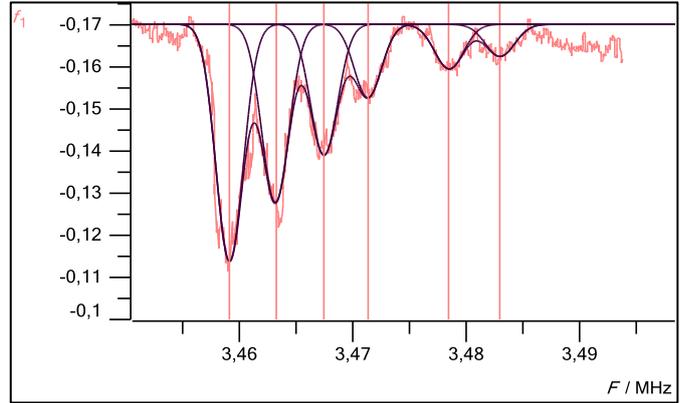
Evaluation

Fig. 7: A spectrum from Fig. 6 with positions of minima.

The positions of the individual transitions are taken from the recorded spectra. They show up as minima in the light intensity.

When irradiated by σ^+ pumping light, the low-frequency transitions of the $F=2$ and $F=1$ groups respectively are the strongest. From the height of the lines it is easy to follow their relative movement, as in Fig. 6. Lines 4 and 5 swap their relative position in the spectrum, as expected from Fig. 4.

The recorded values for the current generating the magnetic field and positions of the lines are given in Table 1

If these values are plotted in a graph as in Fig. 8, apart from the essentially linear dependency, it is not immediately possible to distinguish the splitting into 6 lines.

I	307 mA	490.7 mA	742 mA	888.2 mA
1	3.459 MHz	5.530 MHz	8.356 MHz	9.997 MHz
2	3.463 MHz	5.539 MHz	8.376 MHz	10.025 MHz
3	3.468 MHz	5.548 MHz	8.398 MHz	10.055 MHz
4	3.471 MHz	5.556 MHz	8.419 MHz	10.083 MHz
5	3.478 MHz	5.561 MHz	8.410 MHz	10.065 MHz
6	3.483 MHz	5.570 MHz	8.432 MHz	10.094 MHz

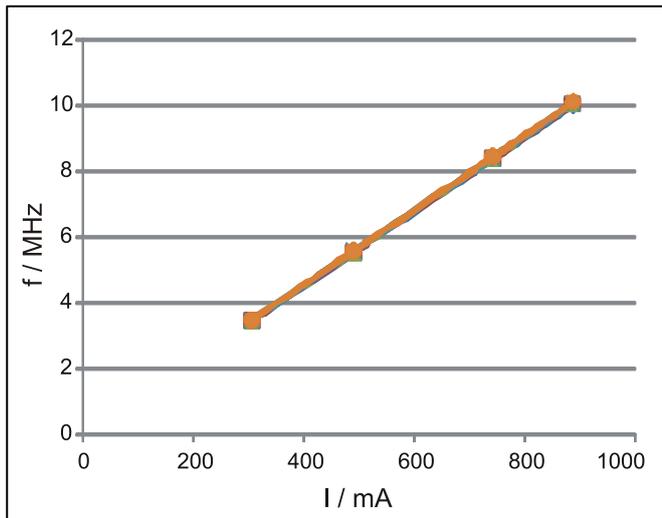Table 1: Position of minima for various currents through the Helmholtz coils.

Fig. 8:   Graph of minima from Table 1

Detail of the splitting of the lines only becomes clear from the graph when the global linear term is subtracted. Theoretically this should be the product of the movement of the average position according to the Breit-Rabi formula and the proportionality between the current and the magnetic field for a set of Helmholtz coils:

6.99 MHz / mT * 1.628 mT / A

However, in practice there exists a degree of discrepancy and the line positions do not change symmetrically.

This is primarily due to the inaccuracy of the current measurement. In the sample measurement, the best fit is obtained for B/I = 1.618 mT / A, i.e. a discrepancy of 0.61%.

The conversion factor between the current and the magnetic field is therefore varied slightly until the splitting of the lines is roughly symmetrical about zero.

I	307 mA	491 mA	742 mA	888 mA
B	0.50 mT	0.79 mT	1.20 mT	1.44 mT
1	-13.3 kHz	-19.9 kHz	-36.0 kHz	-48.7 kHz
2	-8.8 kHz	-11.2 kHz	-15.7 kHz	-20.1 kHz
3	-4.5 kHz	-2.1 kHz	6.3 kHz	9.3 kHz
4	-1.1 kHz	6.7 kHz	26.8 kHz	37.6 kHz
5	6.3 kHz	11.3 kHz	18.0 kHz	20.0 kHz
6	10.8 kHz	19.8 kHz	39.8 kHz	48.9 kHz

Table 2:   Splitting of lines after subtraction of adjusted linear term

What emerges is the picture expected from Fig. 4, with non-linear splitting in accordance with the Breit-Rabi formula.
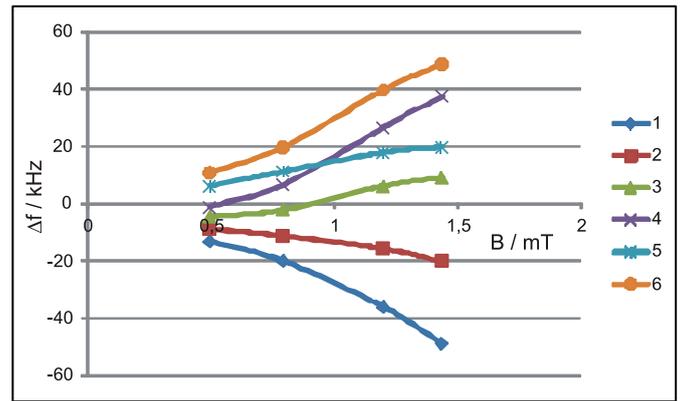

Fig. 9:   Graph of Table 2

Determination of nuclear Landé g-factor g_I

As can be seen from equation (II), the energies of two lines with identical values of m_F but different values of *F* differ only in terms of the sign of the upper term. When the energies are subtracted, then all terms with ξ disappear and only one term $2\dfrac{\mu_K g_I B}{h}$ remains. Matching up the lines between Fig. 4 and Fig. 9, this corresponds to lines 5 and 2 plus 6 and 3 from Table 1.

Δf / MHz	0.50 mT	0.79 mT	1.20 mT	1.44 mT
"5"-"2"	0.0151	0.0225	0.0337	0.0401
"6"-"3"	0.0153	0.0219	0.0335	0.0395

Fitting a straight line to this example results in an average value of 0.0272 MHz/mT

Therefore $2\dfrac{\mu_K g_I B}{h}$

a value of

$|g_I|$ = 1.784

can be derived from this, in comparison to the value quoted in tables, which is

g_I = - 1.827

Literature

[1]   A.Kastler: Journal de Physique, 11 (1950) 255

[2]   H. Kopfermann: Concerning optical pumping of gases, minutes of Heidelberg Academy for Sciences, 1960, 3rd paper

[3]   J. Recht, W. Klein: LH-Contact 1 (1991) S. 8 –11

[4]   G. Breit, I. Rabi: Phys. Rev. 38 (1931) 2002

[5]   Kopfermann, H.: Kernmomente (Nuclear moments), 2nd edition, as of page 28

[6]   S. Penselin: Z.Physik 200 (1967) 467

[7]   C.W.White et al.: Phys.Rev. 174 (1968) 23

[8]   G.H.Fuller et al.: Nuclear Data Tables A5 (1969) 523

[9]   B.N.Taylor et al.: Rev. Mod. Phys. 41 (1969) 375 [9] B.N.Taylor et al.: Rev. Mod. Phys. 41 (1969) 375